Chapter 2

Global structural changes of an ion channel during its gating are reported by ion mobility mass spectrometry

Duygu Yilmaz[a,*], Albert Konijnenberg[b,*], Helgi I. Ingólfsson[a,c], Anna Dimitrova[a], Siewert J. Marrink[a,c], Zhuolun Li[d], Catherine Vénien-Bryan[d], Frank Sobott[b,e] and Armağan Koçer[f]

a Department of Biochemistry, University of Groningen, 9747 AG, Groningen, Netherlands
b Biomolecular & Analytical Mass Spectrometry group, University of Antwerp, Groenenborgerlaan 171, 2020, Antwerp, Belgium
c Zernike Institute for Advanced Materials, University of Groningen, 9747 AG, Groningen, Netherlands
d IMPMC, Sorbonne Universités, CNRS UMR 7590, UPMC Paris 6, 75005 Paris, France
e Center for Proteomics (CFP-CEPROMA), University of Antwerp, Groenenborgerlaan 171, 2020 Antwerp, Belgium
f University Medical Center Groningen, Antonius Deusinglaan 1, 9713AV Groningen, Netherlands

(*) Shared first authorship

Published in Proc. Natl. Acad. Sci. (2014)

Abstract

Mechanosensitive ion channels are sensors probing membrane tension in all kingdoms of life. Despite their importance and vital role in many cell functions, their gating mechanism remains to be elucidated. Here, we studied the gating of MscL by ion mobility mass spectrometry (IM-MS). By screening several detergents for their ability to preserve the oligomeric state of MscL while releasing the protein into the gas phase, we found the conditions that eliminate the need for collisional activation required to free the protein from its protective detergent micelle. We detect the native mass of MscL under these conditions. Next, we reversibly activate the channel and track the structural changes taking place during the channel gating. We trigger MscL into different sub-open intermediate states using heteropentameric MscLs and follow the resulting conformational changes by measuring the rotationally averaged collision cross-sections. Thus, for the first time, we follow MscL gating by IM-MS.

Introduction

Mechanosensitive channel of large conductance (MscL) from *Escherichia coli* is one of the best candidates to explore the gating mechanism of a mechanosensitive channel. The crystal structure of MscL in its closed/nearly closed state from *Mycobacterium tuberculosis* revealed this channel as a homopentamer (Chang *et al.*, 1998). Each subunit has a cytoplasmic N- and C-terminal domain as well as two α-helical transmembrane (TM) domains, TM1 and TM2, which are connected by a periplasmic loop. The five TM1 helices form the pore and the more peripheral TM2 helices interact with the lipid bilayer.

MscL detects changes in membrane tension invoked by a hypo-osmotic shock and couples the tension sensing directly to large conformational changes (Sukharev *et al.*, 1997; Chang *et al.*, 1998). On the basis of a large body of biochemical, crystallography and simulation data, numerous gating models of MscL have been proposed (Blount and Moe, 1999; Yoshimura *et al.*, 1999; Sukharev *et al.*, 2001b; Perozo *et al.*, 2002a; 2002b; Liu *et al.*, 2009; Corry *et al.*, 2010). These models agree on i) the hydrophobic pore constriction of the channel and ii) the opening of the channel by an iris-like rotation: i.e. a tilting and outward movement of transmembrane helices that make the channel wider and shorter (Sukharev *et al.*, 2001b). This mechanism is supported by patch clamp (Sukharev *et al.*, 2001a), disulfide crosslinking (Betanzos *et al.*, 2002), Förster Resonance Energy Transfer (FRET) spectroscopy (Corry *et al.*, 2005), and Site-Directed Spin Labeling Electron Paramagnetic Resonance (SDSL-EPR) experiments (Perozo *et al.*, 2002a; 2002b), as well as computational studies (Gullingsrud and Schulten, 2003; Yefimov *et al.*, 2008; Louhivuori *et al.*, 2010). Short-range local structural changes were reported by these methods, however; the overall global structural changes during channel gating remain to be elucidated. Since there is no crystal structure available for the open MscL channel, elucidating overall global structural changes from the onset of channel activation is of utmost importance for our understanding of the gating mechanism of protein. Here, we combine our ability to activate MscL in a controlled manner to different sub-open states (Birkner *et al.*, 2012), with a native ion mobility-mass spectrometry (IM-MS) approach and provide direct experimental evidence for the key areal changes occurring during channel gating.

Results and Discussion

Micelles formed by detergents with low hydrogen bonding capacity disassemble spontaneously upon transfer into the gas-phase and reveal the embedded pentameric membrane protein, MscL

Native mass spectrometry (MS) relies on the gentle ionization and transfer of intact complexes from solution into the gas-phase by means of nano-electrospray ionization (nanoESI), using desolvation voltages and pressures inside the mass spectrometer that preserve non-covalent interactions (Loo, 1997; Sobott *et al.*, 2002; Heck and van den Heuvel, 2004; Sobott *et al.*, 2005; Hernández and

Robinson, 2007). Together with ion mobility, an adjunct technique that measures collision cross sections and determines the global (rotationally averaged) size of individual particles, native MS is increasingly used to determine the subunit composition, stoichiometry, size, and shape of biomolecular complexes (Ruotolo *et al.*, 2005; 2008; Uetrecht *et al.*, 2010; Konijnenberg *et al.*, 2013). IM-MS has proven exceptionally useful for providing insights also into the structure of membrane proteins, such as subunit stoichiometry and phospholipid interaction with protein components (Barrera *et al.*, 2008; Zhou *et al.*, 2011). Current methodology depends strongly on the apparently protective capabilities of detergent micelles to transfer membrane proteins intact into the vacuum of the mass spectrometer (Barrera *et al.*, 2008; Laganowsky *et al.*, 2013), followed by the removal of these detergents by collisional activation. However, the energy required to rid the membrane protein of its detergent cover often results in the loss of structural integrity of the protein (Borysik *et al.*, 2013; Laganowsky *et al.*, 2013). In order to enable analysis of the native MscL structure by IM-MS (Ruotolo *et al.*, 2005; 2008; Uetrecht *et al.*, 2010; Konijnenberg *et al.*, 2013), we screened several detergents for their ability to preserve and release oligomeric Mscl, hence eliminate the need for collisional activation.

First, we introduced the protein in *n*-dodecyl-β-D-maltoside (DDM) micelles, using nano-ESI, into the mass spectrometer. DDM is one of the most commonly used detergents for native MS of membrane proteins (Barrera and Robinson, 2011). The dissociation of DDM micelles in the gas-phase requires moderate to high levels of collisional activation, i.e. 150V-200V. When using IM-MS to study MscL in DDM, we could only detect monomeric MscL, indicating that these conditions were too harsh to preserve the oligomeric state of MscL (Figure 1A). Next, we tested Triton X-100. Surprisingly, we found that rather than requiring collisional activation to disassemble detergent/protein complexes, oligomers of the protein already appears in the spectra at very mild declustering conditions as a series of pentamer peaks (different charged states) centered around 4750 m/z (Figure 1B). It appears that Triton X-100 micelles dissociate readily in the gas-phase of the mass spectrometer, but we nonetheless detected pentameric MscL with only a few remaining detergent molecules still attached (Figure 1B, enlarged panel).

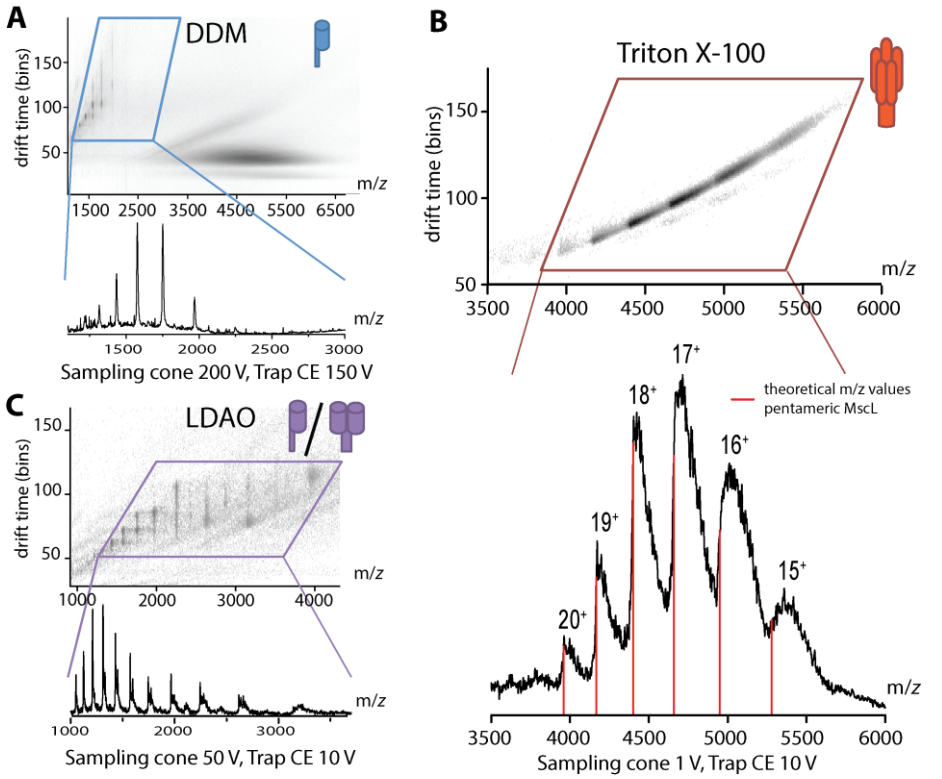

Figure 1. Comparison of the oligomeric states and collisional activation conditions to release MscL from detergent micelles in the gas-phase. (A) Ion mobility spectrum (top) and the excerpt of the mass spectrum in the region where monomeric MscL is observed when released from DDM micelles. Release of MscL from n-dodecyl-β-D-maltoside (DDM) micelles requires high collision energies, which disrupt the MscL pentamer, yielding only monomeric subunits of the protein. **(B)** Ion mobility spectrum (top) and complementary mass spectrum (bottom) of pentameric MscL from Triton X-100 micelles. Triton-100 is not able to generate extensive hydrogen bond networks thus release MscL at much lower collision energies. **(C)** Ion mobility spectrum (top) and the excerpt of the mass spectrum in the region where monomeric and dimeric MscL are observed when released from lauryldimethylamine-oxide (LDAO) micelles.

Upon increasing the collision energy above 30 V to remove the remaining detergent molecules, we found that the energy required partially dissociates MscL in the gas-phase (Figure 2). We therefore kept the various accelerating voltages inside the mass spectrometer below the threshold for dissociation, accepting broader peaks due to the remaining Triton X-100 detergent molecules but avoiding any artefactual structural changes in the protein complex.

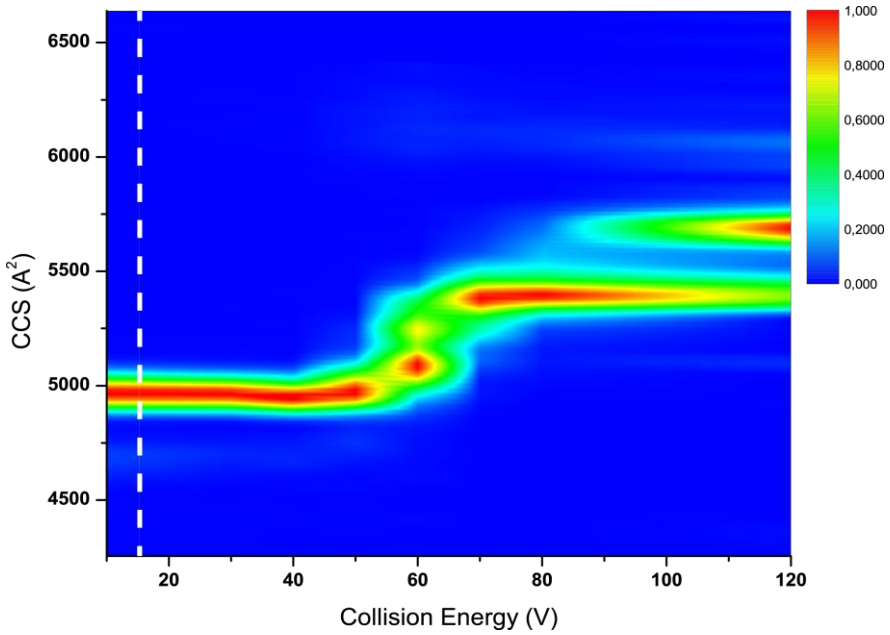

Figure 2. Thermal unfolding of MscL. Heat map representation of thermal unfolding of the 16+ charge state of MscL by increasing the internal energy of the protein due to the more energetic collisions (higher acceleration voltage) with a neutral buffer gas. The dotted white line represents the energy regime used throughout this study.

We explain the ease of protein release from Triton X-100 micelles in the gas-phase by the low hydrogen bond-forming capacity of this detergent compared to DDM. Detergent micelles form in water largely due to the hydrophobic effect, which is absent in the vacuum of the mass spectrometer. For the maltoside-based detergent DDM, a network of hydrogen bonds stabilizes the detergent clusters in the gas-phase, which then require considerable additional energy for dissociation. Triton X-100, on the other hand, is not able to form such an extensive hydrogen bond network, due to its polyethylene oxide head group. Its micelles disassemble spontaneously upon transfer into the gas-phase, thus revealing the embedded oligomeric protein. To test this hypothesis, we screened also pentaethylene glycol monooctyl ether (C8E5) and lauryldimethylamine-oxide (LDAO), which have little possibilities to form an extensive hydrogen bond network. Both C8E5 and LDAO required only 10 V to release the protein from its detergent micelles and the protein was detected in its native pentameric form in C8E5 (data not shown). LDAO micelles required a slightly higher sampling cone voltage of 50 V, but still released MscL at low collision energies and resulted in monomeric/dimeric MscL subunits (Figure 1C). By using detergent micelles that are unstable in the gas-phase, we detect the native mass of MscL by IM-MS. During the preparation of this manuscript, a paper appeared showing that MscL channel from *Mycobacterium*

tuberculosis also keeps its folded conformation in the gas-phase of IM-MS (Laganowsky *et al.*, 2014).

Ion mobility-mass spectrometry can distinguish individual heteropentameric MscL channels by their mass-to-charge ratio and size

Now able to detect pentameric MscL by IM-MS, we set out to follow a range of large global structural changes occurring during MscL gating, i.e. the opening or closing of the channel. In its closed state, the pore diameter is about 3.5 Å (Chang *et al.*, 1998). However, when the channel fully opens, the pore diameter is estimated to become as large as ~30 Å (Cruickshank *et al.*, 1997; van den Bogaart *et al.*, 2007; Wang *et al.*, 2014) which can be detected by IM-MS if it were possible to trigger MscL opening in the absence of the lipid bilayer and tension. Here, in order to open the channel in our experimental setup, we used heteropentameric MscLs comprised of varying number of wild type (WT) and cysteine-point-mutated subunits (G22C) per pentamer (Birkner *et al.*, 2012). Even though in nature MscL opens in response to tension in the lipid bilayer, attaching charged-cysteine specific compounds to the pore of MscL-G22C homopentamers opens the channel spontaneously (Yoshimura *et al.*, 2001; Koçer *et al.*, 2005; 2006). Based on this principle, we gained control on the degree of MscL opening in the absence of tension. We increased the hydrophilicity of the channel pore one subunit at a time, using WT-G22C heteropentameric MscLs. As the number of G22C subunits per heteropentamer increases, hence the number of binding sites for positive charges within the pore constriction, the channels open further and visit higher subconducting states (Birkner *et al.*, 2012).

We first tested any conformational differences in individual heteropentameric channels in their closed form using IM-MS. We generated homo- (WT_5 and $G22C_5$) and heteropentameric (WT_4G22C_1, WT_3G22C_2, WT_2G22C_3) channels using a duet expression system, as described previously (Birkner *et al.*, 2012). Briefly, two *mscL* genes (WT-MscL with a StrepII-tag and G22C-MscL with a 6His-tag) were cloned and co-expressed in *E. coli* PB104, which allowed the production of homo- and heteropentameric channel assemblies in the host cell membrane. Individual heteropentamers were then obtained by using a three-step purification protocol; two-step affinity chromatography to remove the homopentameric MscL, followed by chromatofocussing to separate the individual heteropentameric MscL based on their isoelectric points (pI) (Figure 3).

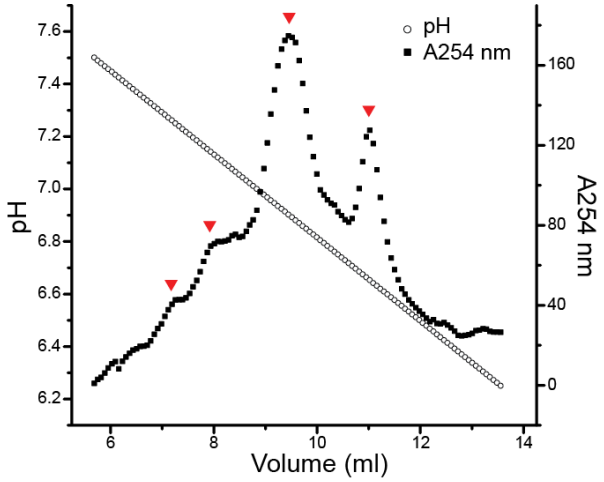

Figure 3. Chromatofocussing profile. MscL heteropentamers with different numbers of WT-StrepII and G22C-6His subunits differ in their surface isoelectric point (pI). The normalized chromatogram shows four peaks representing the individual populations: WT_1G22C_4, WT_2G22C_3, WT_3G22C_2 and WT_4G22C_1 (from left to right).

Using IM-MS, we determined the mass to charge ratio and the rotationally averaged size (collision cross section, CCS) of individual pentamers (Table 1). The CCS was found to increase slightly with the number of WT subunits within a given hetero-pentamer. This observation was attributed to the larger size of the StrepII-tag of WT monomers relative to the size of the 6His-tag. Indeed, IM-MS of the homopentameric WT MscL channels with StrepII-tag gave a larger CCS than the same protein with 6His-tag (Table 1).

	Masses		Closed states	
	Theoretical (Da)	Observed (Da)	CCS (A^{o2})	CCS tag corrected (A^{o2})
WT-6His	78255	78342±29	4861±61	-
WT-StrepII	79345	79461±32	4927±59	-
WT_4G22C_1	79173	79182±37	4944±64	4959±64
WT_3G22C_2	79001	79114±45	4917±59	4947±59
WT_2G22C_3	78829	78882±42	4902±63	4948±63
$G22C_5$	78485	78600±15	4884±63	4960±63

Table 1. IM-MS allows for size determination of different homo- and heteropentamers. The small difference in measured CCS of MscL pentamers can be correlated to the difference in purification tags.

MscL gating can be detected reversibly by ion mobility-mass spectrometry

In order to see whether the gating of MscL can be detected by IM-MS, we first showed the covalent binding of a positively-charged cysteine-specific channel activator [2-(trimethylammonium)ethyl] methanethiosulfonate bromide (MTSET) to cysteines of the G22C subunits (Figure 4).

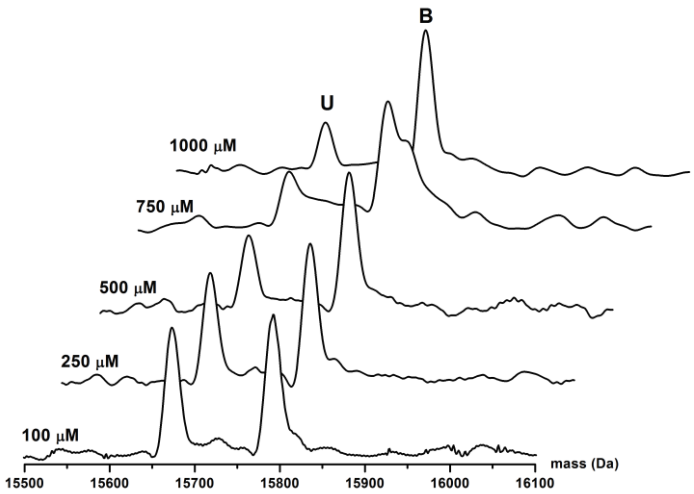

Figure 4. Titration of $G22C_5$ MscL with MTSET. MscL-labeling by MTSET was assessed after dissociation of the protein complex in the gas-phase, as the mass difference induced by MTSET binding was too small to observe in native mass spectrometry, given the polydispersity of protein-detergent complex. The spectra show the ratio of MscL monomers with (B) and without (U) MTSET covalently attached. The MscL subunits were not stoichiometrically labeled despite the specific reactivity of MTSET for cysteines; the maximal degree of labeling was reached with 750μM MTSET. It is possible that further labeling of the five cysteine sites in the pore lining is limited by the already introduced positive charge, *i.e.* the introduction of 2-(trimethylammonium)ethyl moieties upon labeling with MTSET.

We tested increasing amounts of MTSET with $G22C_5$ homopentamer and showed that MTSET concentrations above 500 μM maximally label the cysteines (beyond 1000 μM MTSET causes deterioration of the IM-MS signal occurs due to ion suppression). Therefore, routinely, we used 750 μM MTSET for activating MscL channels.

Next, we measured the rotationally averaged collision cross-section (CCS) of the $G22C_5$ homopentamer in the presence of 750 μM MTSET (Figure 5A). The closed channel had a CCS centered round 4960±63 $Å^2$ (CCS ± range). After MTSET treatment, the CCS of $G22C_5$ increased and showed four distinct peaks at 5095±46, 5330±48, 5580±56 and 5890±106 $Å^2$ (CCS ± range), suggesting various sub-open

conformations of the channel. To prove that the presence of MTSET had opened the channel, we added the reducing agent, DTT, to reverse the labeling by MTSET and show that the CCS returned back to its original value (Figure 5A). We also tested the effect of the MTSET on wild type MscL and show that it did not cause any changes in the CCS. This is the first time that ion channel gating is observed by employing IM-MS to monitor global conformational changes.

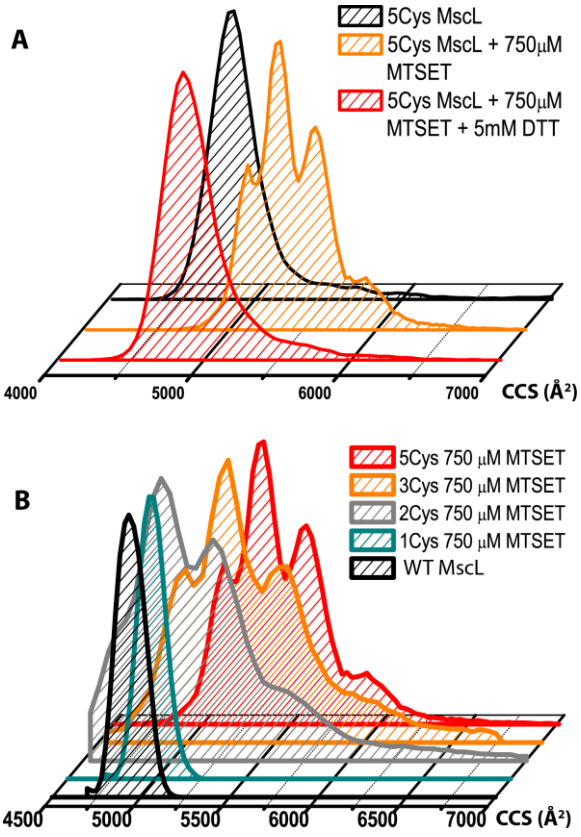

Figure 5. (A) Charge-induced opening of MscL is reversible upon removal of the charge from the pore lining by reduction of the disulfide bond between the cysteine and MTSET. The shift and dispersity of the collision cross section observed for the 16+ charge state of $G22C_5$ MscL upon binding of MTSET indicates opening of the channel. After adding DTT to the same sample, the channel returns to its closed state again **(B) Opening of MscL observed by ion mobility mass spectrometry.** Increasing the number of MTSET-labeled cysteines in the pore lining allows MscL to occupy more extended conformations, as well as the frequency of occupation of these conformations. Reported collision cross sections are corrected for the different compositions of the purification tags of the heteropentamers of MscL.

The overall size of MscL channels increases as the hydrophilicity of the pore increases

Finally, we could resolve the channel opening to different subopen states by activating heteropentameric MscLs with varying number of MTSET-labeled G22C subunits. When WT_4G22C_1 was activated with MTSET, no detectable change in CCS was observed using IM-MS (Figure 5B). However, patch clamp electrophysiology (Birkner *et al.*, 2012), dual-color fluorescence (Mika *et al.*, 2013), and fluorescence dequenching assays (Figure 6) showed conductance through the WT_4G22C_1/MTSET channel pore. The maximum pore opening for this heteropentamer was calculated to be up to 15 Å (Mika *et al.*, 2013). Introducing a second charge in the pore, using MTSET activated WT_3G22C_2 mutant, on the other hand, generated two major CCS populations averaged around 5266±64 $Å^2$ and 5557±98 $Å^2$ (CCS ± range) (Figure 5B), indicating that MscL already goes through at least two pronounced conformational states in its journey from its closed to the two-charge activated state. With the addition of the third charge to the pore, i.e. WT_2G22C_3 activated with MTSET, the channel visited the same extended conformations as WT_3G22C_2 MscL but with higher frequency (Figure 5B). Homopentameric $G22C_5$, when activated with MTSET, displayed all intermediate CCSs that were also observed for the heteropentameric forms of MscL, but also showed an additional more compact (5095±46 $Å^2$) and a more extended (5890±106 $Å^2$) conformation. These findings are in good agreement with the patch clamp single channel measurements of individual heteropentamers when activated by MTSET (Birkner *et al.*, 2012). While WT_4G22C_1 visits a very low conducting state with 2% probability and stays mainly in the closed conformation (Probability density, P = 98%), as the number of MTSET attached subunits increases, the channel visits higher sub-conducting states and presents a more flickering behavior (Mika *et al.*, 2013). Homopentameric $G22C_5$, activated with MTSET, spends most of its time in the early substates, while it visits the closed form only 25% of the time according to this data. Therefore, in a given time, $G22C_5$ channels give the highest resolution, that might explain the smallest conformational change of 5095 $Å^2$ being visible in $G22C_5$ but not in WT_4G22C_1. Overall, IM-MS could detect multiple conformations of MscL during its gating between the closed and the open forms (Figure 5B).

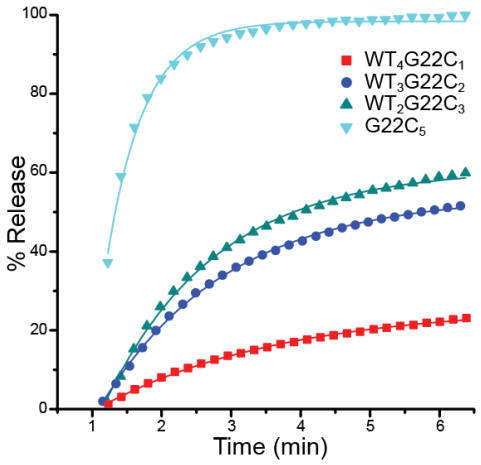

Figure 6. Fluorescence dequenching assay. Homo- and heteropentamers of MscL were assayed by a fluorescence dequenching assay. The net percent release of liposomal fluorophore content was calculated from the increase in fluorescence after activating the channel with 1 mM final concentration of MTSET. Single exponential efflux rate constants are kWT_4G22C_1 = 0.38±0.08 min^{-1}, kWT_3G22C_2 = 0.55±0.03 min^{-1}, kWT_2G22C_3 = 0.62±0.04 min^{-1}, $kG22C_5$ = 1.84±0.02 min^{-1}.

MTSET-induced increase in the size of MscL obtained by IM-MS corresponds with that of tension activated channel in molecular dynamics simulations

In order to correlate observed (changes in) sizes of rotationally averaged collision cross-sections of charge-activated MscL as determined by IM-MS with tension-induced MscL gating, we performed coarse-grained molecular dynamics simulations. Using the closed state crystal structure of MscL from *M. tuberculosis* (Chang *et al.*, 1998; Steinbacher *et al.*, 2007) a coarse-grained model (Yefimov *et al.*, 2008; Louhivuori *et al.*, 2010) was generated and embedded in a 1,2-dioleoyl-*sn*-glycero-3-phosphocholine (DOPC) bilayer. By applying tension (65 dyn/cm) on the membrane, we were able to simulate initial channel opening. In the first ~100 ns following the application of the lateral bilayer tension, the MscL transmembrane helices tilted, extending the extracellular cavity and flattening the channel in the plane of the bilayer (Figure 7A). The channel took an additional ~200 ns before the channel pore expanded enough to allow water permeation through the pore (Figure 7B). The onset of water flux through the channel correlates well with the observed increase in minimum pore radius (Figure 7C). Figure 7D shows the calculated CCS for various time points of the simulation. The CCS gradually increased from a value of ~4900 $Å^2$ before the tension was applied, to about 5200 - 5300 $Å^2$ when the channel gates, and reaches its first sub-states, corresponding well with the cross section values of the closed (4960 $Å^2$) and first two expanded conformation (5095 and 5330 $Å^2$) as determined by the IM-MS experiments (Figure 5). These findings further support that the observed very early, hence compact, conformations seen for the charge activated MscL pass through similar sub-states as tension-activated MscL in its transitions from the closed to the open conformation (Birkner *et al.*, 2012).

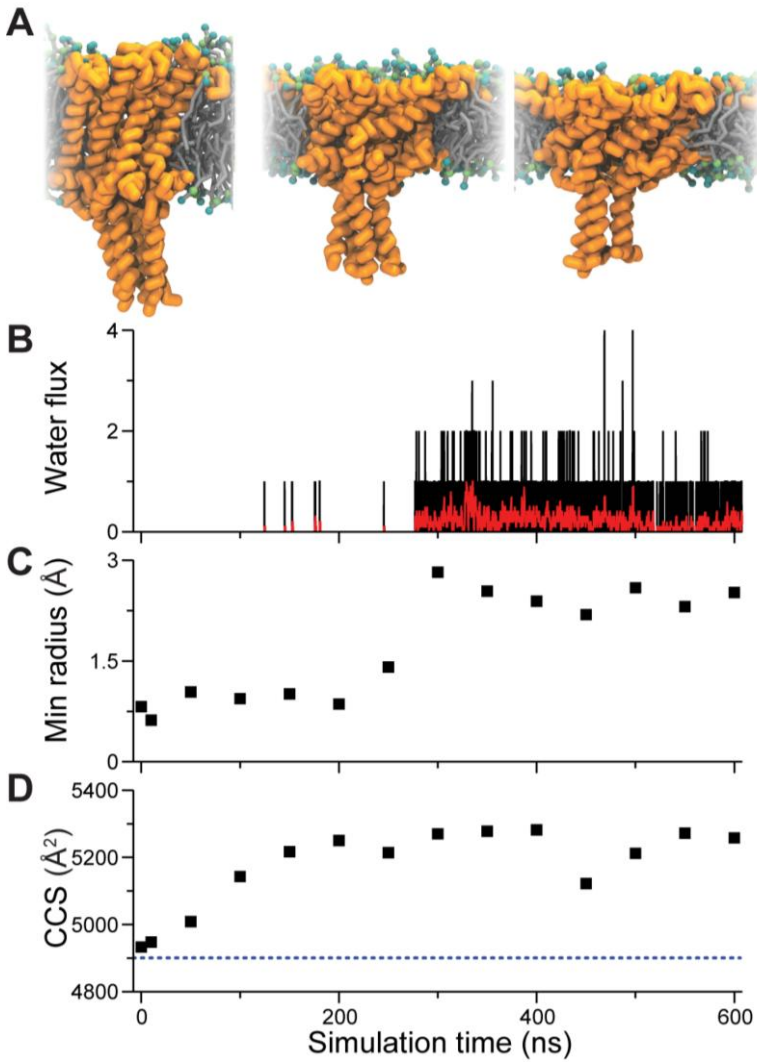

Figure 7. MscL gated with applied tension in MD simulations. (A) Snapshots from a Martini coarse-grained MD simulation show how the opening of the channel is governed by tilting of the helix bundle in response to flattening of the membrane (from left to right: no tension, with tension after 100 ns and 300 ns). After applying bilayer tension the water flux through the channel was monitored **(B)**; showing flux per 0.15 ns (black) and average over 3 ns (red). **(C)** Minimum pore radius through the pore constriction (residues 12-25) **(D)** shows the CCS calculated from the MD simulations.

Structural changes during MscL gating are intrinsic to the protein

The observed enlargement of heteropentamers with increasing number of MTSET-bound subunits also suggest that MscL can open in the absence of a lipid bilayer. Previously, charge-induced activation of MscL has been shown in intact *E. coli* cells (Betanzos *et al.*, 2002; Bartlett, 2004), in spheroplasts (Corry *et al.*, 2005; Bartlett *et al.*, 2006), and with reconstituted systems (Perozo *et al.*, 2002a; 2002b; Yoshimura *et al.*, 2008). In all of these cases MscL was embedded in a lipid bilayer environment. To support our IM-MS findings, we studied MscL channels in Triton X-100 with and without MTSET, using both electron paramagnetic resonance (EPR) spectroscopy and electron microscopy. Together with site–directed spin labeling (SDSL), EPR provides information on protein structure and dynamics both in detergent and in lipid bilayers (Hubbell *et al.*, 2000). To make MscL visible for EPR, we specifically and partially (50% spin labeling efficiency) labeled homopentameric G22C mutant with 1–oxyl–2,2,5,5–tetramethylpyrrolin–3–yl)methyl methane thiosulfonate (MTSSL). The G22 position of MscL has been previously shown to change its environment when the channel opens (Perozo *et al.*, 2002a; 2002b). We monitored structural changes of MscL in Triton X-100 by following the variations in spin-spin interactions, and the mobility of the spin labels within MscL as a function of MTSET activation of the channel (Figure 8). If the channel opens, the distance between the spin labels increases and causes a change in the EPR line-shape, and an increase in the mobility of the spin labels. The overall line broadening in the absence of MTSET indicated closer proximity between spin labels (i.e., stronger spin-spin interaction) in the closed form (Figure 8, black trace). However, upon MTSET treatment, broadening disappeared (Figure 8, red trace); suggesting that the subunits of MscL moved farther apart. Furthermore, interaction with MTSET increased the probe mobility (Figure 8).

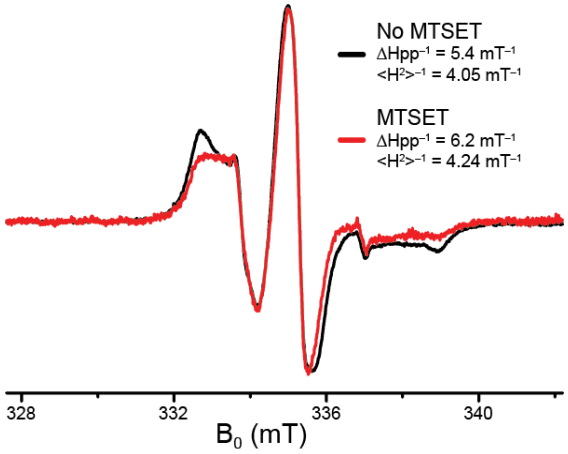

Figure 8. CW-EPR spectra of spin–labeled G22C MscL solubilized in Triton X-100 at room temperature. MscL was partially labeled at its 22nd amino acid position with a cysteine-specific spin probe MTSSL with the labeling efficiency of 50%). EPR spectra were normalized to maximum amplitude and correspond to 36 accumulations (black trace: no MTSET, red trace: with MTSET; protein concentration of 285 μM). Two EPR parameters are used to assess the mobility of the spin probe quantitatively: the mobility parameter (the inverse of the central line width, $_{\Delta}Hpp^{-1}$) and the inverse of the second moment ($<H^2>^{-1}$). An increase in the spin label motional freedom is reflected in an increase of both numerical values and is associated with channel opening. In the absence of MTSET the values were: $_{\Delta}Hpp^{-1}$ = 5.4 mT^{-1}; $<H^2>^{-1}$ = 4.05 mT^{-1}, whereas in the presence of MTSET: $_{\Delta}Hpp-1$ = 6.2 mT^{-1}; $<H^2>^{-1}$ = 4.24 mT^{-1}. This indicates that upon MTSET binding, detergent solubilized MscL opens in the absence of a lipid bilayer environment.

Next, we employed transmission electron microscopy and image analysis to study the closed (no MTSET) and partially open (750 μM MTSET) states of $G22C_5$ MscL in Triton X-100 detergent micelles. Negatively stained closed and partially open MscL channels appear as bright spots as shown in Figure 9A in the left and right panel, respectively. Using WEB and SPIDER software packages, 1403 closed and 1004 open state, centered and aligned channel images were averaged. In its closed form, the area of the averaged MscL images in detergent was 5007 $Å^2$ (Figure 9B left panel). Upon treatment with MTSET, the channels became flatter and wider and expanded to 6165 $Å^2$ (Figure 9B right panel). Even though we took the averaged images as a measure, we were able to classify open and closed channels into different sub-classes using the WEB and SPIDER software (Figure 9 C-F). While Figure 9 C and D shows the three classes in the closed form of MscL from the top and the side, respectively, E and F shows three classes of the open state from the top and side, respectively. The observed subclasses may represent different sub-closed and sub-open states. Furthermore, the EM data on the averaged images of the closed and partially open state with a 27±5% area increase upon MTSET

opening, which is in good agreement with the CCS increase found by IM-MS of 21±3%. Together, the EM data strongly supports that our conclusion from IM-MS that MscL gates in the absence of detergent or membrane lipids.

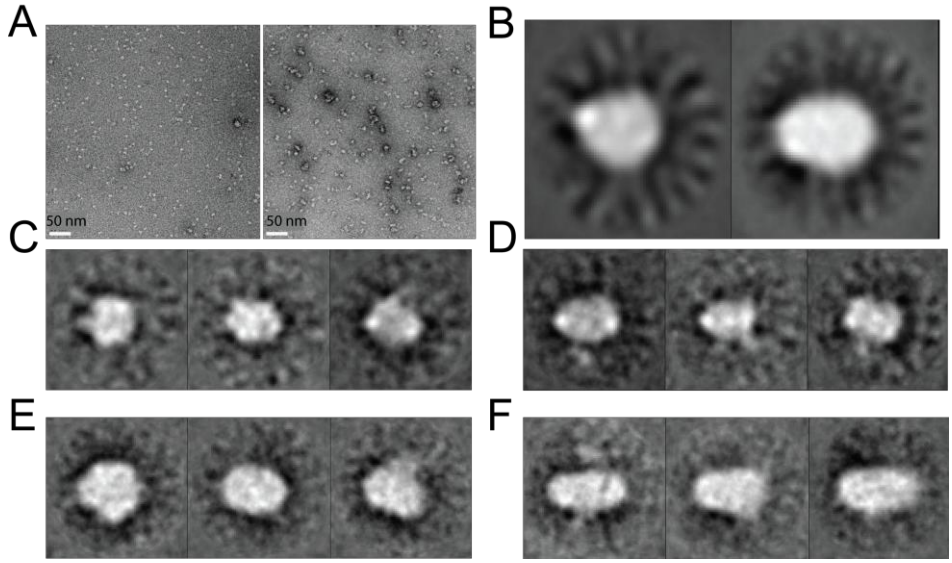

Figure 9. Electron micrograph and image processing of MscL closed and open states. Closed state or open state MscL was applied at a concentration of about 0.03 mg/ml to electron microscope grids and stained with 2% uranyl acetate. **(A)** Electron micrographs of negatively-stained MscL. Left: closed state. Right: open state. The particles appear white on a darker background. **(B)** Image averaging of MscL. Left: Image averaging of 1403 closed state particles (centered and aligned) Right: Image averaging of 1004 different partially opened channels (centered and aligned). **(C-F)** Gallery of selected classes of MscL molecules. **(C-D)** Closed state MscL C: three classes showing the top views D: three classes showing the side view. **(E-F)** Open state MscL: E: three classes showing the top view D: three classes showing the side view. The size of the box is 212 Å x 212 Å.

In conclusion, detergent micelles that require minimum energy for their disassembly in the gas-phase are valuable tools for the study of membrane proteins by native IM-MS. Resolving the global shape of MscL in combination with its mass-to-charge ratio made it possible to follow the global structural chances of MscL upon its gating. The method could detect as small as a 3% change in the rotationally-averaged collision cross-sections of the protein complex from the closed (4952 $Å^2$) to the first detectable substate of 5095 $Å^2$. We believe this approach opens new avenues for further studies on the dynamic structures of membrane proteins, which were so far unattainable by other methods.

Materials and Methods

Sample preparation and native IM-MS

MscL homo- and heteropentamers were produced as described elsewhere (Koçer *et al.*, 2007; Birkner *et al.*, 2012) and solubilized in detergent at 2x critical micelle concentration. Proteins at 5-20 μM were buffer exchanged (Superdex 200 column) into 100 mM ammonium acetate pH 6.8 and introduced without further desalting into the mass spectrometer using nanoESI with gold-coated borosilicate capillaries at capillary voltages of 1.2-1.6 kV. Spectra were recorded in positive ion mode on a commercially available traveling wave ion mobility mass spectrometer, Synapt G2 HDMS (Waters) with 32k quadrupole and settings optimized for transmission of large complexes. Gas pressures were 6.0 mbar, $8.35e^{-3}$ mbar, $3.26e^{-2}$ mbar and 1.31 mbar for backing, source, trap and the ion mobility cell, respectively, and He and IMS cell gas flows were 60 and 30 ml/min respectively. Critical voltages for intact transmission of the detergent/protein complexes were found to be low sampling and extraction cone voltages (1 and 1 V, respectively), with trap and transfer collision energies (CE) set to 10 and 3.5 V and the trap cell bias to 35 V, unless otherwise stated.

Homo- and heteropentamer samples were incubated for 5 min at room temperature with the indicated concentrations of MTSET prior to analysis. A series of different incubation times revealed that after 5 min no further opening was observed, which is in good agreement with the fast and specific nature of MTSET binding to cysteine residues. Experimental CCS obtained by IM-MS were calibrated against proteins of known cross section such as cytochrome C, β-lactoglobulin, albumin, alcohol dehydrogenase and glutamate dehydrogenase, as reported previously (Barrera *et al.*, 2008; Bush *et al.*, 2010; Laganowsky *et al.*, 2013). All reported cross sections are from one of the lowest observed charge states (16+), as it represents the most native conformation. The m/z scale of all mass spectra was externally calibrated using a 10 mg/ml CsI solution. The spectra were processed using Masslynx 4.1.

MD simulations

Simulations of MscL gating were performed using the Martini coarse-grain (CG) model (Marrink *et al.*, 2004; 2007; Monticelli *et al.*, 2008) and the GROMACS 4.x simulation package (Hess *et al.*, 2008) following a similar protocol as described previously (Yefimov *et al.*, 2008; Louhivuori *et al.*, 2010). In short, the topology of MscL was derived from the crystal structure of the closed state Tb-MscL (PDB ID 2OAR) (Chang *et al.*, 1998; Steinbacher *et al.*, 2007) using CG Martini 2.0. The channel was solvated in 562 CG 1,2-dioleoyl-sn-glycero-3-phosphocholine (DOPC) lipids and around 20k CG water beads (corresponding to about 80k water molecules) using the *insane.py* script. The temperature and pressure were controlled using the Berendsen thermostat (298 K) and barostat (Berendsen *et al.*, 1984). The initial system was energy-minimized (steepest descent, 500 steps) and

simulated for 1 ns using short time step 1-10 fs simulations and with position restrains on the protein backbone. The restrains were released, the time step set to 30 fs and the system was equilibrated for 4 μs with 1 bar semi-isotropic pressure coupling. Bilayer tension was incrementally applied in seven short (3 ns) simulations to a value of 65 dyn/cm and then simulated for 0.6 μs. In the first ca. 100 ns following the application of the lateral bilayer tension and thinning of the bilayer, the MscL transmembrane helixes tilted, extending the extracellular cavity of the channel. The channel hydrophobic gate takes an additional ca. 200 ns before expanding and opening the channel. Selected frames from the CG simulation were back-mapped into atomistic coordinates using the Wassenaar *et al.* reverse transformation method (Wassenaar *et al.*, 2014) and minimised with the GROMOS 54a7 force field (Schmid *et al.*, 2011). The minimum pore radius was measured for the same backmapped frames using the HOLE 2.0 program (Smart *et al.*, 1993). The radius was defined as the radius of the largest sphere that could pass through the channel hydrophobic lock (-0.5 to 1 nm along the channel pore axes starting from the centre of mass of residue 18) and interacting with the fully atomistic structure using their van der Waals radii.

All CCS calculations were done using MOBCAL (Mesleh *et al.*, 1996; Shvartsburg and Jarrold, 1996) with the projection approximation (PA) algorithm at 298 K and He as a buffer gas. To correct for the use of N_2 in the IM-MS experiments and the underestimation of cross sections by the PA algorithm, all calculated CCS were scaled by the experimentally derived factor of 1.14 (Hall *et al.*, 2012). Simulations snapshots were generated using the molecular graphics viewer VMD (Humphrey *et al.*, 1996).

EPR spectroscopy

Continuous wave (CW) EPR measurements were performed using a commercially available MiniScope benchtop X-band EPR spectrometer (MS400 Magnettech GmbH, Berlin, Germany) with a rectangular TE102 resonator. The microwave power was set to 10 mW and the B-field modulation amplitude to 0.20 mT. EPR glass capillaries (0.9 mm inner diameter) were filled with sample volume of 50 μL with a final protein concentration of 285 μM. The microwave frequency was 9.41 GHz and the modulation frequency was 100 kHz. Each spectrum corresponds to the accumulation of 36 scans.

Electron microscopy

0.03 mg/ml MscL in 100 mM ammonium acetate pH 6.8 buffer was applied in its closed or partially open state, i.e. activated by MTSET, to electron microscope grids and stained with 2% uranyl acetate. The specimens were analyzed with a JEOL 2100, LaB_6 operating at 200kV. A Gatan CCD camera was used (4kx4k, pixel size 15 Å) for collecting the data. Micrographs were recorded at a nominal magnification of 40,000 (pixel size was 2.65Å). The WEB and SPIDER software packages (Frank *et al.*, 1996) were used for image processing. 1403 particles in the closed state and

1004 particles in the partially open states were picked by hand, windowed, subjected to reference free alignment, and sorted into classes using the K-means clustering (Frank, 1990). Each class contained images of particles viewed from the same orientation.

Chromatofocussing

Heteropentamers of MscL were separated by chromatofocussing as described before (Birkner *et al.*, 2012). Briefly, a Mono P 5/200 GL chromatofocussing column (GE Healthcare) was equilibrated with 20 mL start buffer (25 mM Tris-acetic acid (pH 8.3) at 10 °C, 10 mM NaCl, 0.2% (v/v) Triton X-100), and a pre-gradient was formed by washing the column with 6 mL of elution buffer pH:5.0 (7 mL Polybuffer 74, 3 mL Polybuffer 96, 10 mM NaCl, 0.2% (v/v) Triton X-100). The hetero-pentamer mixture was desalted prior to application to the chromatofocussing column by using a NAP-10 column. During elution, 250-µL fractions were collected. The pH of the fractions was determined at 6 °C. The protein content of the peak fractions was determined by using a 2-D Quant Kit (GE Healthcare) according to the manufacturer's protocol.

Fluorescence dequenching assay

Proteins were reconstituted into synthetic liposomes according to Koçer *et al.* (Koçer *et al.*, 2007) Briefly, azolectin was thawed and sized by extrusion 11 times through a 400 nm filter. The resulting liposomes were destabilized by the addition of Triton X-100. Protein and lipids were mixed at 1:50 weight ratio and incubated for 30 min at 50 °C. Subsequently, self-quenching dye solution (200 mM calcein in 10 mM sodium phosphate (pH 8.0)) was added at a 1:1 volume ratio, and was supplemented with 6 mg (wet weight) Biobeads (SM-2 absorbents; Bio-Rad) per microliter of detergent (10% Triton X-100) used in the sample and lipid preparation. For detergent removal, the sample was incubated overnight (ca. 16 h) at 4 °C under mild agitation. The proteoliposomes were applied to a Sephadex G50 Pharmacia size-exclusion column to remove the free dye. All elution fractions were assayed in a Varian Cary Eclipse fluorometer at an excitation wavelength of 495 nm and the emission recorded at 515 nm. In a standard assay, 3 µL calcein-filled proteoliposomes were diluted into 2.2 mL efflux buffer. At t = 1 min, MTSET was added at a final concentration of 1 mM for channel activation. The fluorescence was measured continuously, and the total fluorescence of the sample was determined by dissolving the proteoliposomes with 0.5% (v/v) Triton X-100 at t = 7 min. The datasets were normalized by taking the initial fluorescence of each sample as 0% and the signal after the Triton X-100 addition as 100%. The data was fitted to the exponential plot and the first-order rate constants (k) and SD values for calcein efflux were calculated for each heteropentamer.

References

Barrera, N.P., and Robinson, C.V. (2011). Advances in the Mass Spectrometry of Membrane Proteins: From Individual Proteins to Intact Complexes. Annu. Rev. Biochem. *80*, 247–271.

Barrera, N.P., Di Bartolo, N., Booth, P.J., and Robinson, C.V. (2008). Micelles Protect Membrane Complexes from Solution to Vacuum. Science *321*, 243–246.

Bartlett, J.L. (2004). An in vivo assay identifies changes in residue accessibility on mechanosensitive channel gating. Proc. Natl. Acad. Sci *101*, 10161–10165.

Bartlett, J.L., Li, Y., and Blount, P. (2006). Mechanosensitive Channel Gating Transitions Resolved by Functional Changes upon Pore Modification. Biophys. J. *91*, 3684–3691.

Berendsen, H.J.C., Postma, J.P.M., van Gunsteren, W.F., DiNola, A., and Haak, J.R. (1984). Molecular dynamics with coupling to an external bath. J. Chem. Phys. *81*, 3684–3690.

Betanzos, M., Chiang, C.-S., Guy, H.R., and Sukharev, S. (2002). A large iris-like expansion of a mechanosensitive channel protein induced by membrane tension. Nat. Struct. Biol. *9*, 704–710.

Birkner, J.P., Poolman, B., and Koçer, A. (2012). Hydrophobic gating of mechanosensitive channel of large conductance evidenced by single-subunit resolution. Proc. Natl. Acad. Sci *109*, 12944–12949.

Blount, P., and Moe, P.C. (1999). Bacterial mechanosensitive channels: integrating physiology, structure and function. Trends Microbiol. *7*, 420–424.

Borysik, A.J., Hewitt, D.J., and Robinson, C.V. (2013). Detergent Release Prolongs the Lifetime of Native-like Membrane Protein Conformations in the Gas-Phase. J. Am. Chem. Soc. *135*, 6078–6083.

Bush, M.F., Hall, Z., Giles, K., Hoyes, J., Robinson, C.V., and Ruotolo, B.T. (2010). Collision Cross Sections of Proteins and Their Complexes: A Calibration Framework and Database for Gas-Phase Structural Biology. Anal. Chem. *82*, 9557–9565.

Chang, G., Spencer, R.H., Lee, A.T., Barclay, M.T., and Rees, D.C. (1998). Structure of the MscL homolog from Mycobacterium tuberculosis: a gated mechanosensitive ion channel. Science *282*, 2220–2226.

Corry, B., Hurst, A.C., Pal, P., Nomura, T., Rigby, P., and Martinac, B. (2010). An improved open-channel structure of MscL determined from FRET confocal microscopy and simulation. J. Gen. Physiol. *136*, 483–494.

Corry, B., Rigby, P., Liu, Z.-W., and Martinac, B. (2005). Conformational Changes Involved in MscL Channel Gating Measured using FRET Spectroscopy. Biophys. J. *89*, L49–L51.

Cruickshank, C.C., Minchin, R.F., Le Dain, A.C., and Martinac, B. (1997). Estimation of the pore size of the large-conductance mechanosensitive ion channel of Escherichia coli. Biophys. J. *73*, 1925–1931.

Frank, J. (1990). Classification of macromolecular assemblies studied as "single particles." Q. Rev. Biophys. *23*, 281–329.

Frank, J., Radermacher, M., Penczek, P., Zhu, J., Li, Y., Ladjadj, M., and Leith, A. (1996). SPIDER and WEB: Processing and Visualization of Images in 3D Electron Microscopy and Related Fields. J. Struct. Biol. *116*, 190–199.

Gullingsrud, J., and Schulten, K. (2003). Gating of MscL studied by steered molecular dynamics. Biophys. J. *85*, 2087–2099.

Hall, Z., Politis, A., Bush, M.F., Smith, L.J., and Robinson, C.V. (2012). Charge-State Dependent Compaction and Dissociation of Protein Complexes: Insights from Ion Mobility and Molecular Dynamics. J. Am. Chem. Soc. *134*, 3429–3438.

Heck, A.J.R., and van den Heuvel, R.H.H. (2004). Investigation of intact protein complexes by mass spectrometry. Mass Spectrom. Rev. *23*, 368–389.

Hernández, H., and Robinson, C.V. (2007). Determining the stoichiometry and interactions of macromolecular assemblies from mass spectrometry. Nat. Protoc. *2*, 715–726.

Hess, B., Kutzner, C., van der Spoel, D., and Lindahl, E. (2008). GROMACS 4: Algorithms for Highly Efficient, Load-Balanced, and Scalable Molecular Simulation. J. Chem. Theory Comput. *4*, 435–447.

Hubbell, W.L., Cafiso, D.S., and Altenbach, C. (2000). Identifying conformational changes with site-directed spin labeling. Nat. Struct. Biol. *7*, 735–739.

Humphrey, W., Dalke, A., and Schulten, K. (1996). VMD: Visual molecular dynamics. J. Mol. Graphics Modell. *14*, 33–38.

Koçer, A., Walko, M., and Feringa, B.L. (2007). Synthesis and utilization of reversible and irreversible light-activated nanovalves derived from the channel protein MscL. Nat. Protoc. *2*, 1426–1437.

Koçer, A., Walko, M., Bulten, E., Halza, E., Feringa, B.L., and Meijberg, W. (2006). Rationally Designed Chemical Modulators Convert a Bacterial Channel Protein into a pH-Sensory Valve. Angew. Chem. Int. Ed. *45*, 3126–3130.

Koçer, A., Walko, M., Meijberg, W., and Feringa, B.L. (2005). A Light-Actuated Nanovalve Derived from a Channel Protein. Science *309*, 755–758.

Konijnenberg, A., Butterer, A., and Sobott, F. (2013). Native ion mobility-mass spectrometry and related methods in structural biology. Biochim. Biophys. Acta (BBA) - Proteins and Proteomics *1834*, 1239–1256.

Laganowsky, A., Reading, E., Allison, T.M., Ulmschneider, M.B., Degiacomi, M.T., Baldwin, A.J., and Robinson, C.V. (2014). Membrane proteins bind lipids selectively to modulate their structure and function. Nature *510*, 172–175.

Laganowsky, A., Reading, E., Hopper, J.T.S., and Robinson, C.V. (2013). Mass spectrometry of intact membrane protein complexes. Nat. Protoc. *8*, 639–651.

Liu, Z., Gandhi, C.S., and Rees, D.C. (2009). Structure of a tetrameric MscL in an expanded intermediate state. Nature *461*, 120–124.

Loo, J.A. (1997). Studying Noncovalent Protein Complexes by Electrospray Ionization Mass Spectrometry. Mass Spectrom. Rev. 1–23.

Louhivuori, M., Risselada, H.J., van der Giessen, E., and Marrink, S.J. (2010). Release of content through mechano-sensitive gates in pressurized liposomes. Proc. Natl. Acad. Sci *107*, 19856–19860.

Marrink, S.J., de Vries, A.H., and Mark, A.E. (2004). Coarse Grained Model for Semiquantitative Lipid Simulations. J. Phys. Chem. B *108*, 750–760.

Marrink, S.J., Risselada, H.J., Yefimov, S., Tieleman, D.P., and de Vries, A.H. (2007). The MARTINI Force Field: Coarse Grained Model for Biomolecular Simulations. J. Phys. Chem. B *111*, 7812–7824.

Mesleh, M.F., Hunter, J.M., Shvartsburg, A.A., Schatz, G.C., and Jarrold, M.F. (1996). Structural Information from Ion Mobility Measurements: Effects of the Long-Range Potential. J. Phys. Chem. *100*, 16082–16086.

Mika, J.T., Birkner, J.P., Poolman, B., and Koçer, A. (2013). On the role of individual subunits in MscL gating: "All for one, one for all?." FASEB J. *27*, 882–892.

Monticelli, L., Kandasamy, S.K., Periole, X., Larson, R.G., Tieleman, D.P., and Marrink, S.J. (2008). The MARTINI Coarse-Grained Force Field: Extension to Proteins. J. Chem. Theory Comput. *4*, 819–834.

Perozo, E., Cortes, D.M., Sompornpisut, P., Kloda, A., and Martinac, B. (2002a). Open channel structure of MscL and the gating mechanism of mechanosensitive channels. Nature *418*, 942–948.

Perozo, E., Kloda, A., Cortes, D.M., and Martinac, B. (2002b). Physical principles underlying the transduction of bilayer deformation forces during mechanosensitive channel gating. Nat. Struct. Biol. *9*, 696–703.

Ruotolo, B.T., Benesch, J.L.P., Sandercock, A.M., Hyung, S.-J., and Robinson, C.V. (2008). Ion mobility–mass spectrometry analysis of large protein complexes. Nat. Protoc. *3*, 1139–1152.

Ruotolo, B.T., Giles, K., Campuzano, I., Sandercock, A.M., Bateman, R.H., and Robinson, C.V. (2005). Protein Interaction in the Gaseous Phase. Science *2005*, 1658–1660.

Schmid, N., Eichenberger, A.P., Choutko, A., Riniker, S., Winger, M., Mark, A.E., and Gunsteren, W.F. (2011). Definition and testing of the GROMOS force-field versions 54A7 and 54B7. Eur. Biophys. J. *40*, 843–856.

Shvartsburg, A.A., and Jarrold, M.F. (1996). An exact hard-spheres scattering model for the mobilities of polyatomic ions. Chem. Phys. Lett. *261*, 86–91.

Smart, O.S., Goodfellow, J.M., and Wallace, B.A. (1993). The pore dimensions of gramicidin A. Biophys. J. *65*, 2455–2460.

Sobott, F., Hernández, H., McCammon, M.G., Tito, M.A., and Robinson, C.V. (2002). A Tandem Mass Spectrometer for Improved Transmission and Analysis of Large Macromolecular Assemblies. Anal. Chem. *74*, 1402–1407.

Sobott, F., McCammon, M.G., Hernandez, H., and Robinson, C.V. (2005). The flight of macromolecular complexes in a mass spectrometer. Phil. Trans. R. Soc. a: Mathematical, Physical and Engineering Sciences *363*, 379–391.

Steinbacher, S., Bass, R., Strop, P., and Rees, D.C. (2007). Structures of the Prokaryotic Mechanosensitive Channels MscL and MscS. In Current Topics in Membranes, (Elsevier), pp. 1–24.

Sukharev, S., Betanzos, M., Chiang, C.S., and Guy, H.R. (2001a). The gating mechanism of the large mechanosensitive channel MscL. Nature *409*, 720–724.

Sukharev, S., Durell, S.R., and Guy, H.R. (2001b). Structural Models of the MscL Gating Mechanism. Biophys. J. *81*, 917–936.

Sukharev, S.I., Blount, P., Martinac, B., and Kung, C. (1997). Mechanosensitive channels of Escherichia coli: the MscL gene, protein, and activities. Annu. Rev. Physiol. *59*, 633–657.

Uetrecht, C., Rose, R.J., van Duijn, E., Lorenzen, K., and Heck, A.J.R. (2010). Ion mobility mass spectrometry of proteins and protein assemblies. Chem. Soc. Rev. *39*, 1633–1655.

van den Bogaart, G., Krasnikov, V., and Poolman, B. (2007). Dual-Color Fluorescence-Burst Analysis to Probe Protein Efflux through the Mechanosensitive Channel MscL. Biophys. J. *92*, 1233–1240.

Wang, Y., Liu, Y., DeBerg, H.A., Nomura, T., Hoffman, M.T., Rohde, P.R., Schulten, K., Martinac, B., and Selvin, P.R. (2014). Single molecule FRET reveals pore size and opening mechanism of a mechano-sensitive ion channel. eLife *3*, e01834–e01834.

Wassenaar, T.A., Pluhackova, K., Böckmann, R.A., Marrink, S.J., and Tieleman, D.P. (2014). Going Backward: A Flexible Geometric Approach to Reverse Transformation from Coarse Grained to Atomistic Models. J. Chem. Theory Comput. *10*, 676–690.

Yefimov, S., van der Giessen, E., Onck, P.R., and Marrink, S.J. (2008). Mechanosensitive Membrane Channels in Action. Biophys. J. *94*, 2994–3002.

Yoshimura, K., Batiza, A., and Kung, C. (2001). Chemically Charging the Pore Constriction Opens the Mechanosensitive Channel MscL. Biophys. J. *80*, 2198–2206.

Yoshimura, K., Batiza, A., Schroeder, M., Blount, P., and Kung, C. (1999). Hydrophilicity of a single residue within MscL correlates with increased channel mechanosensitivity. Biophys. J. *77*, 1960–1972.

Yoshimura, K., Usukura, J., and Sokabe, M. (2008). Gating-associated conformational changes in the mechanosensitive channel MscL. Proc. Natl. Acad. Sci *105*, 4033–4038.

Zhou, M., Morgner, N., Barrera, N.P., Politis, A., Isaacson, S.C., Matak-Vinkovic, D., Murata, T., Bernal, R.A., Stock, D., and Robinson, C.V. (2011). Mass Spectrometry of Intact V-Type ATPases Reveals Bound Lipids and the Effects of Nucleotide Binding. Science *334*, 380–385.